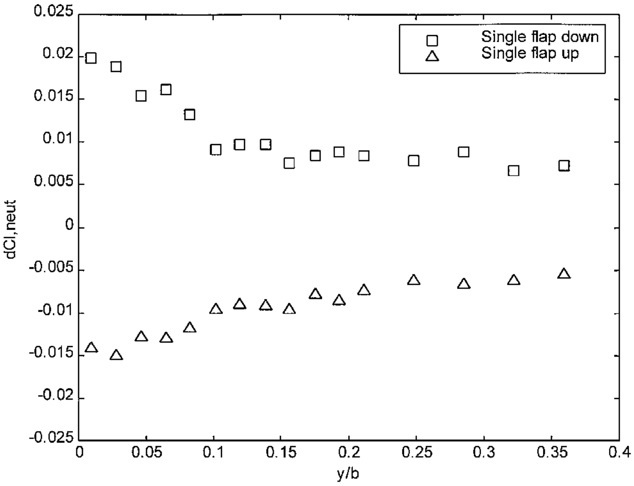

Fig. 4 Streamwise pressure profiles at midspan for single flaps at α = 0.40 deg.

incidences, as shown in Fig. 2a. The pitching-moment trends are the same as those observed for the lift.

Because of this linear response with flap span, the superposition of flap effects was examined. Near 0-deg incidence the loads were measured in a great variety of flap configurations, including situations where actuated flaps were nonadjacent. The lift response vs b_{down}/b was identical to Fig. 3, regardless of the whether the actuators were adjacent or not, demonstrating that responses can be superposed.

The effects of single flaps were examined, with MiTEs applied at various spanwise positions. The loads response was independent of actuator position, as the measured lift and pitching moment changed by the same amount (within measurement uncertainty) for all flap locations. The midspan pressure profiles were used to determine how the loads varied with the position of the actuated MiTE. Figure 4 shows the midspan C_l relative to the neutral position as a function of the actuated flap location. As expected, the strongest effects are found when the actuated flap is aligned with the row of pressure taps. However, as the applied flap grows more distant, the response does not decay to zero, showing an influence as much as 10 flap spans away.

Conclusions

The loads response of miniature trailing-edge flaps has been studied over a variety of static conditions. Full-span tests indicate that the airfoil lift and pitching moment at a given angle of attack can be considerably altered, which implies that MiTEs are capable of the significant loads changes necessary for control. The small gaps between MiTEs (5% of the actuator span) cause no notable performance degradation. Partial-span tests about midspan show a linear response with changes in flap span, a result that should simplify control design. The load responses can also be superposed, even if the actuators are not adjacent to each other. Finally, single flaps exhibit a spanwise influence at least 10 flap spans away, demonstrating a considerable nonlocal effect. This could be an issue with designing a control system, as the MiTE concept was devised in the hopes that each flap could influence the loads at a particular section. Although the strongest effects are directly at the flap, they are clearly not limited to a small spanwise region. Overall, these experiments have shown that MiTEs are good candidates for the development of a system for damping active aeroelastic instabilities.

Acknowledgments

This work is sponsored by the U.S. Air Force Office of Scientific Research. Collaborations with Ilan Kroo, Fritz Prinz, and Byong-ho Park were critical to the research.

References

[1]Kroo, I. M., "Aerodynamic Concepts for Future Aircraft," AIAA Paper 99-3524, June 1999.

[2]Storms, B. L., and Jang, C. S., "Lift Enhancement of an Airfoil Using a Gurney Flap and Vortex Generators," *Journal of Aircraft*, Vol. 31, No. 3, 1994, pp. 542–547.

[3]Liebeck, R. H., "Design of Subsonic Airfoils for High Lift," *Journal of Aircraft*, Vol. 15, No. 9, 1978, pp. 547–561.

[4]Myose, R., Papadakis, M., and Heron, I., "Gurney Flap Experiments on Airfoils, Wings, and Reflection Plane Model," *Journal of Aircraft*, Vol. 35, No. 2, 1998, pp. 206–211.

[5]Yen-Nakafuji, D. T., van Dam, C., Michel, J., and Morrison, P., "Load Control for Turbine Blades: A Non-Traditional Microtab Approach," AIAA Paper 2002-0054, Jan. 2002.

[6]Park, B., "Miniaturization of Functional Mechanisms with SDM Processing," Ph.D. Dissertation, Dept. of Mechanical Engineering, Stanford Univ., Stanford, CA, Jan. 2002.

[7]Solovitz, S. A., "Experimental Aerodynamics of Mesoscale Trailing-Edge Actuators," Ph.D. Dissertation, Dept. of Mechanical Engineering, Stanford Univ., Stanford, CA, Dec. 2002.

A. Plotkin
Associate Editor

Effect of the Initial Conditions on Turbulent Boundary Layers

David J. Walker* and Luciano Castillo†
Rensselaer Polytechnic Institute, Troy, New York 12180

I. Introduction

THERE have been a number of recent developments of great interest in turbulent boundary layers. First, Castillo[1] and Castillo and George[2] analyzed the Reynolds-averaged Navier–Stokes (RANS) equations using equilibrium similarity analysis. They showed that the mean velocity profiles could be Reynolds-number invariant in the limit of infinite Reynolds number only if in the same limit the outer velocity scale were proportional to the freestream velocity U_∞. The mean deficit profile according to the analysis by George and Castillo[3] for zero pressure gradient (ZPG) and the similarity analysis of Castillo and George[2] for pressure gradient (PG) then should scale with U_∞ and is given by

$$(U_\infty - U)/U_\infty = f_{\text{op}}(\bar{y}, \delta^+, \Lambda, *) \tag{1}$$

The arguments inside the similarity function f_{op}, are the outer similarity coordinate $\bar{y} = y/\delta_{99}$, the Reynolds-number dependence $\delta^+ = \delta u_*/\nu$, the pressure gradient parameter Λ, and any possible dependence on the upstream conditions $*$, respectively. The pressure gradient parameter Λ was determined via similarity analysis using the RANS equations and is given by

$$\Lambda \equiv -\frac{\delta}{U_\infty\, \mathrm{d}\delta/\mathrm{d}x}\frac{\mathrm{d}U_\infty}{\mathrm{d}x} = \text{constant} \tag{2}$$

In the limit as $Re \to \infty$, Eq. (1) is independent of the Reynolds number. However, at finite Reynolds number the function f_{op} depends on both the upstream conditions and the local Reynolds number. Moreover, George and Castillo[3] were not able to completely collapse the data with just U_∞ for ZPG boundary layers and attributed this failure to the local Reynolds-number effects. Second, Zagarola and Smits[4] found an empirical velocity scale $U_\infty\delta_*/\delta$ that did successfully collapse the data for the outer flow ($\bar{y} \geq 0.1$) of ZPG turbulent boundary

Received 22 December 2000; presented as Paper 2001-2912 at the Fluids 2001 Conference, Anaheim, CA, 11–14 June 2001; revision received 26 July 2002; accepted for publication 26 July 2002.

*Graduate Student, Department of Mechanical Engineering, Aeronautical and Mechanics.

†Assistant Professor, Department of Mechanical Engineering, Aeronautical Engineering and Mechanics. Member AIAA.

layers given as

$$\frac{U_\infty - U}{U_\infty \delta_* / \delta} = F_0(\bar{y}) \tag{3}$$

Notice, that the preceding function F_0 is independent of the local Reynolds number and the upstream conditions.

Subsequently, Wosnik and George[5] showed that this scaling was consistent with the theory of George and Castillo[3] for ZPG boundary layers. Third, it was shown by Castillo,[6] Castillo et al.,[7] and Castillo and Walker[8] that using the Zagarola and Smits scaling the Reynolds-number dependence of PG boundary layers is removed and that it yields to three profiles in turbulent boundary layers: one for favorable pressure gradient (FPG), one for adverse pressure gradient (APG), and one for ZPG. This is true even for boundary layers near and at separation. However, Castillo and Walker[8] were unable to demonstrate how the upstream conditions affect the development of the downstream flow, particularly on the outer mean velocity profiles.

Therefore, the main focus of this Note is to show that the mean deficit profiles collapse with just U_∞ for fixed upstream conditions, but to different curves depending on the upstream conditions (i.e., wind-tunnel speed) and strength of the pressure gradient. In addition, it will be shown that using the Zagarola and Smits scaling the upstream dependence is removed.

II. Mean Velocity Profiles

To understand the importance of the upstream conditions in the downstream flow, we will first look at the velocity deficit profiles normalized by U_∞ for fixed upstream conditions, and then we will compare the same data but normalized with the Zagarola/Smits scaling $U_\infty \delta_* / \delta$. Castillo[6] and Castillo et al.[7] showed a great amount of data in cases where the upstream conditions were not fixed, including boundary layers near and at separation.

Figure 1 shows the velocity deficit profiles normalized by U_∞ and δ_{99} for the ZPG (top), FPG (center), and APG (bottom) turbulent boundary layers. The ZPG measurements for fixed upstream conditions of Castillo and Johansson,[9] Wieghardt,[10] and Smith and Walker[11] are plotted together in the top figure. The data of Castillo and Johansson, Wieghardt, and Smith and Walker will be referred to as CJ, WT, and SW, respectively, from now on. The ZPG measurements of CJ were performed for a fixed wind-tunnel speed U_0 of 10 m/s, whereas WT profiles were performed for a fixed upstream velocity U_0 of 33 m/s. Finally, the profiles from SW are shown for a fixed upstream velocity of 52 m/s. Notice that the three profiles vary from low to high Reynolds number, and yet the profiles collapse individually for fixed upstream conditions, but to different curves. Moreover, the difference in the profiles is caused by the variation in the upstream conditions. In addition, as the wind-tunnel speed increases the profiles move toward the wall.

The FPG deficit profiles (center) of Fig. 1 show the moderate FPG data of Ludwieg and Tillmann,[12] the mild FPG data of Herring and Norbury,[13] and the moderate FPG data of Schubauer and Klebanoff,[14] respectively. (The data from Schubauer and Klebanoff are taken from the airfoil in the FPG region only.) The mean deficit profiles are normalized by U_∞ and δ_{99}. The data of Ludwieg and Tillmann, Herring and Norbury, and Schubauer and Klebanoff will be referred to as LT, HN, and SK, respectively, from now on. There are some important results that follow from these figures. First, the velocity profiles each collapse individually for two different strength of pressure gradients (mild and moderate FPG), except the profile of HN, which shows a reasonable collapse. Second, the wind tunnel speed U_0 is different for all three experiments: 11.5 m/s for LT, 23.3 m/s for HN, and 30.7 m/s for SK. Also, notice that the FPG profiles from HN and LT nearly collapse with one another, but the data from SK are slightly different. Moreover, the influence on the upstream conditions on the FPG profiles is not as significant as it was for the ZPG profiles.

The bottom of Fig. 1 shows various APG experiments plotted together. The moderate APG data of Clauser[15] and the mild and moderate APG data of Bradshaw[16] are shown in the same figure normalized by U_∞ and δ_{99}. The wind-tunnel speed is different in each case; 7.96 m/s for Clauser at moderate, 41.6 m/s for Bradshaw at moderate, and 43.7 m/s for Bradshaw at mild APG. All three profiles collapse individually over a range of Reynolds number from low to moderately high, thus showing that these APG profiles are Reynolds-number invariant for fixed upstream conditions. Also, notice that the moderate APG data of Bradshaw and Clauser, both with the same strength of PG and the same range of Reynolds-number collapse, but to different curves. The only difference between these two profiles is the upstream conditions (i.e., wind-tunnel speed). The moderate APG data of Bradshaw have a wind-tunnel speed of 41.6 m/s, whereas the Clauser data have a wind-tunnel speed of 7.96 m/s.

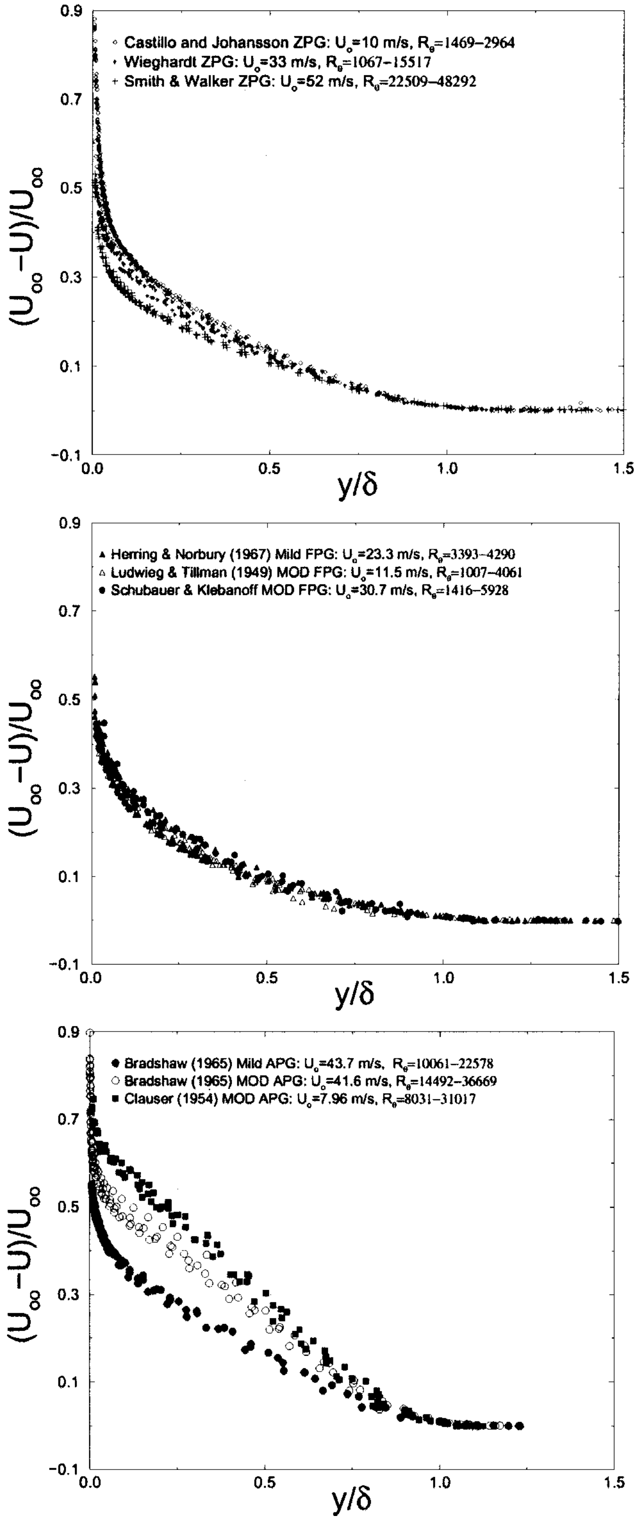

Fig. 1 Velocity deficit profiles for ZPG (top), FPG (middle), and APG (bottom) normalized by U_∞ and δ_{99}.

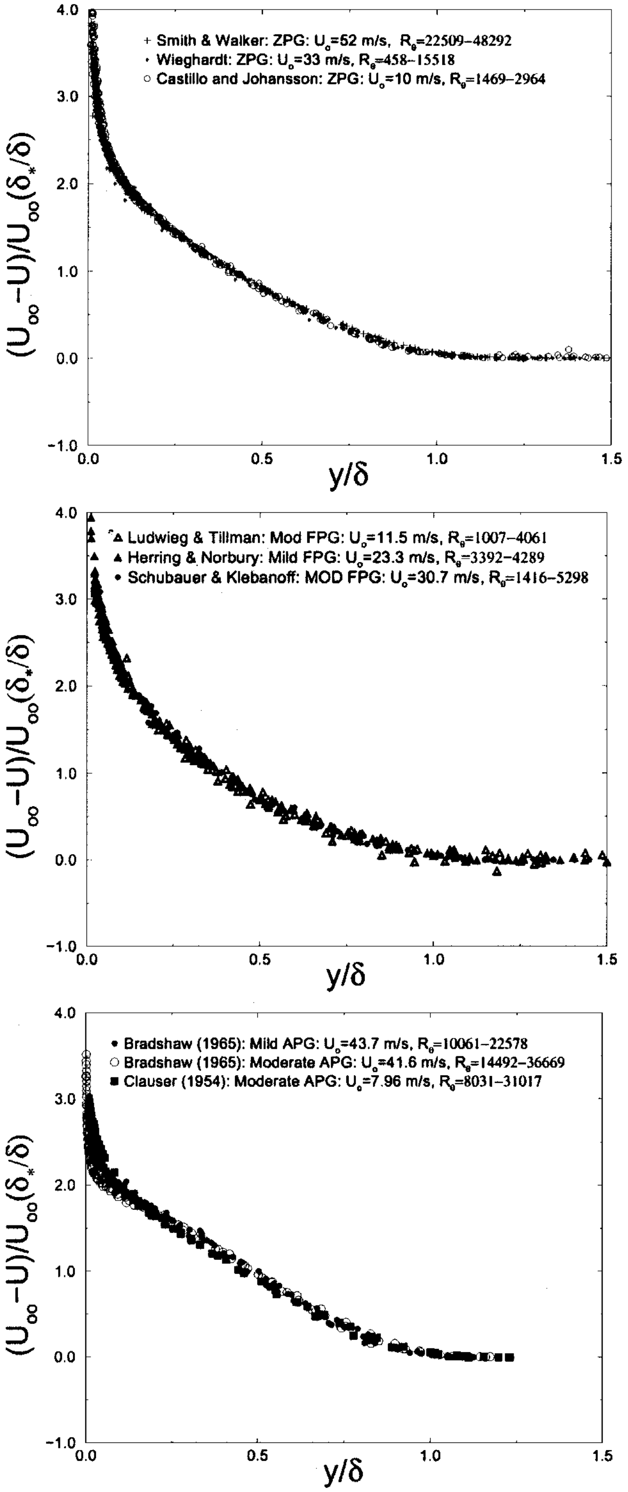

Fig. 2 Velocity deficit profiles normalized by $U_\infty(\delta_*/\delta_{99})$ and δ_{99}. Top panel shows the ZPG profiles, middle panel shows the FPG profiles, and bottom panel shows the APG.

Furthermore, notice that the difference between the profiles is more evident in APG than in FPG or ZPG. Also, as the wind-tunnel speed decreases from 43.7 to 7.96 m/s in APG the profiles move away from the wall. Traditionally, we would have expected that profiles with the same range of Reynolds number and same strength of pressure gradient would collapse to the same curve. However, the mean deficit profiles for the ZPG, FPG, and APG of Fig. 1 show the opposite. It is clear that the effect of the upstream conditions play an important role in the shape of the profiles. The difference shown between the profiles for the FPG is not nearly as evident as in ZPG and APG, but it is there.

Figure 2 shows the ZPG, FPG, and APG profiles of Fig. 1 but now normalized by the Zagarola/Smits scaling $U_\infty\delta_*/\delta_{99}$. Again, the ZPG profiles are shown at the top, the FPG at the center, and the APG at the bottom. It is clear that all of the upstream dependence is completely removed from the profiles; thus, the mean deficit profiles collapse to a single curve and the shape of the profiles is unique for ZPG, FPG, and APG. This is consistent with the work of Castillo and George, who stated that there could only be three profiles in turbulent boundary layers: one for ZPG, one for FPG, and one for APG. Therefore, the parameter δ_*/δ contains the upstream dependence $*$ of the outer flow.

III. Conclusions

This work laid the foundation for understanding how the upstream conditions affect the downstream flow in turbulent boundary layers. It was shown that for fixed upstream conditions (i.e., fixed wind-tunnel speed) the mean velocity deficit profiles collapse with just U_∞ but each to a different curve. In addition, the strength of the PG also affects the shape of the profile. Moreover, flows with even the same strength of PG and same range of Reynolds-number collapse, but to different curves depending on the upstream conditions. Furthermore, the influence of the upstream conditions in the downstream flow is more pronounced in APG than for the FPG and ZPG flows. In addition, the ratio of δ_*/δ in the Zagarola and Smits scaling contains the effect of the upstream conditions. The fact that in APG boundary layers the upstream conditions play an important role in the shape of profiles might help us to explain why many turbulence models have failed to characterize boundary layers.

References

[1]Castillo, L., "Similarity Analysis of Turbulent Boundary Layers," Ph.D. Dissertation, Dept. of Mechanical Engineering, State Univ. of New York, Buffalo, NY, Feb. 1997.

[2]Castillo, L., and George, W. K., "Similarity Analysis for Turbulent Boundary Layer with Pressure Gradient: Outer Flow," *AIAA Journal*, Vol. 39, No. 1, 2001, pp. 41–47.

[3]George, W. K., and Castillo, L., "Zero-Pressure Gradient Turbulent Boundary layer," *Applied Mechanics Reviews*, Vol. 50, No. 11, Pt. 1, 1997, pp. 689–729.

[4]Zagarola, M. V., and Smits, A. J., "Mean-Flow Scaling of Turbulent Pipe Flow," *Journal of Fluid Mechanics*, Vol. 373, 1998, pp. 33–79.

[5]Wosnik, M., and George, W. K., "Reconciling the Zagarola/Smits Scaling with the George/Castillo Theory for the Zero Pressure Gradient Turbulent Boundary Layer," AIAA Paper 2000-0911, Jan. 2000.

[6]Castillo, L., "Application of Zagarola/Smits Scaling in Turbulent Boundary Layers with Pressure Gradient," *Advances in Fluids Mechanics 3*, edited by M. Raham and C. A. Brebbia, Vol. 26, WIT Press, Boston, 2000, pp. 275–288.

[7]Castillo, L., Walker, D. J., and Wosnik, M., "The Effect of the Upstream Conditions on the Mean Velocity Deficit of Turbulent Boundary Layers," AIAA Paper 2000-2309, June 2000.

[8]Castillo, L., and Walker, D., "The Effect of the Upstream Conditions on the Outer Flow of Turbulent Boundary Layers," *AIAA Journal*, Vol. 40, No. 7, 2002, pp. 1292–1299.

[9]Castillo, L., and Johansson, T. G., "The Effects of the Upstream Conditions in a Low Reynolds Number Turbulent Boundary Layer with Zero Pressure Gradient," *Journal of Turbulence* (to be published).

[10]Wieghardt, K., "Über die Wandschubspannung in Turbulenten Reibungsschichten bei Veränderlichem Aussendruck," Kaiser Wilhelm Inst. für Strömungsforschung, No. UM-6603, Göttingen, Germany, 1943.

[11]Smith, D. W., and Walker, J. H., "Skin-Friction Measurements in Incompressible Flow," NACA Rept. R 26, 1959.

[12]Ludwieg, H., and Tillmann, W., "Investigations of the Wall Shearing Stress in Turbulent Boundary Layers," NACA TM 1285, 1950.

[13]Herring, H., and Norbury, J., "Some Experiments on Equilibrium Turbulent Boundary Layers in Favorable Pressure Gradients," *Journal of Fluid Mechanics*, Vol. 27, 1967, pp. 541–549.

[14]Schubauer, G. B., and Klebanoff, P. S., "Investigation of Separation of the Turbulent Boundary Layer," NACA TR 1030, 1951.

[15]Clauser, F. H., "The Turbulent Boundary Layer," *Advances in Applied Mechanics*, Vol. 4, 1954, pp. 1–51.

[16]Bradshaw, P., "The Turbulence Structure of Equilibrium Boundary Layers," NPL Aero. Rept. 1184, 1966.

H. M. Atassi
Associate Editor